View metadata, citation and similar papers at core.ac.uk

brought to you by CORE

provided by Elsevier - Publisher Connector

Available online at www.sciencedirect.com

SciVerse ScienceDirect

Procedia CIRP 6 (2013) 594 – 599

www.elsevier.com/locate/procedia

The Seventeenth CIRP Conference on Electro Physical and Chemical Machining (ISEM)

Parametric effects on grit embedment and surface morphology in an innovative hybrid waterjet cleaning process for alpha case removal from titanium alloys

L. Huang[a]*, P. Kinnell[a], P.H. Shipway[b]

[a] *Manufacturing Research Division, Faculty of Engineering, The University of Nottingham, University Park, Nottingham, NG7 2RD, UK*
[b] *Materials, Mechanics and Structures Research Division, Faculty of Engineering, The University of Nottingham, University Park, Nottingham, NG7 2RD, UK*

* Corresponding author. Tel.: +44 (0)115 951 4034; fax: +44 (0)115 951 3800. *E-mail address*: epxlh3@nottingham.ac.uk.

Abstract

An innovative hybrid waterjet cleaning (HWJC) process which aims to combine the benefits of both abrasive waterjet (AWJ) and plain waterjet (PWJ) processes has been proposed in this paper as an innovative solution for bulk removal of thick alpha case from titanium alloys. In the HWJC process, AWJ is firstly applied to the target surface in order to remove the surface material to a near-desired depth; the PWJ operation is then applied to clean the AWJ-machined surface. The PWJ process is designed to remove the embedded abrasive particles from the AWJ-machined surface and to provide a polishing effect (reduction in surface roughness). In order to evaluate the performance of HWJC, a series of experimental runs have been conducted on Ti-6Al-4V with an alpha case layer. The influence of PWJ processing parameters on the efficiency of grit removal was examined. The results showed that the HWJC process can effectively reduce the area coverage of grit contamination. However, the grit removal efficiency is dependent not only on the operating parameters of the PWJ, but also upon the embedment behavior of the abrasive particles.

© 2013 The Authors. Published by Elsevier B.V. Open access under CC BY-NC-ND license.
Selection and/or peer-review under responsibility of Professor Bert Lauwers

Keywords: Waterjet cleaning, grit embedment, grit removal, alpha case removal.

Nomenclature

WJ	waterjet	Ra	arithmetic mean deviation of the surface roughness (μm)
AWJ	abrasive waterjet	v	jet traverse speed (mm/min)
PWJ	plain waterjet	SO	Step over (mm)
HWJC	hybrid waterjet cleaning	SOD	standoff distance (mm)
SEM	scanning electron microscopy	θ	jet impingement angle (°)
BS	backscattered	DoR	depth of removal
EDX	energy dispersive X-ray	n	number of jet passes
AG	area percentage of garnet grit	f_a	abrasive flow rate
MRR	material removal rate (mm^3/min)		

1. Introduction

As a promising non-conventional machining method, high pressure waterjet technology has found its use in cutting, milling, cleaning and other applications. It has advantages over other machining technologies, such as it no thermal effect on the workpiece, environmental friendliness, versatility and flexibility. There are generally two types of waterjet technology, namely abrasive waterjet (AWJ) and plain waterjet (PWJ). AWJ makes use of a high-pressure waterjet discharged from an orifice in combination with fine abrasive particles (i.e. garnet) to machine target materials by means of erosion, while PWJ consists of high-pressure waterjet without any abrasives.

2212-8271 © 2013 The Authors. Published by Elsevier B.V. Open access under CC BY-NC-ND license.
Selection and/or peer-review under responsibility of Professor Bert Lauwers
doi:10.1016/j.procir.2013.03.077

Although abrasive grit can significantly enhance the erosive removal of materials, industrial applications in waterjet surface treatment usually prefer to use PWJ as AWJ results in grit embedment into the workpiece surface, which is not acceptable in many situations. It was shown that the AWJ through-cut surface on Ti-6Al-4V and A286 steel exhibited poor fatigue behavior compared with a laser through-cut surface due to the role of embedded grit acting as a crack initiator [1]. Chen *et al.* [2] also argued that grit contamination may generate serious problems for further treatment of these surfaces such as welding or coating, in addition to its negative impact on the fatigue resistance.

With increasing operating pressure of waterjet pumps available in the market (i.e. up to 620 MPa), plain waterjet is now capable of machining extremely hard materials, with initial attempts having been reported by several researchers [3-5]. A major concern with PWJ machining of hard materials is its relatively low material removal rate (MMR) as compared to the AWJ process. However, processing of hard materials using PWJ is still attractive for certain applications in the aerospace, automotive and medical industries due to its specific characteristics.

To sum up, AWJ can remove material quickly but tends to result in grit contamination of the treated surface, whilst PWJ results in surfaces free of grit embedment, but with a sacrifice in erosion efficiency. Attempting to solve this dilemma, an innovative hybrid waterjet cleaning process (HWJC) aiming to combine the benefits of both processes has been proposed in this paper as a solution for bulk removal of thick alpha case using waterjet technology. In the HWJC process, AWJ is first applied to the target surface to remove the surface material to a near-desired depth, followed by PWJ of the same area. The PWJ process is designed to remove any embedded grit particles left by the AWJ process, and also provide a 'polishing' effect to the AWJ-machined surface to improve the surface topography. Examples of machining strategies for the HWJC process are shown in Fig.1.

In order to evaluate the performance of the HWJC process, quantification of grit embedment on HWJC-treated surfaces was examined. Although a considerable amount of research investigating grit embedment in blasting and AWJ machining has been conducted [2, 6-11], efforts have focused on understanding of the role of process parameters in determining the degree of grit embedment; existing studies have not focused on secondary grit-removal operations.

In this paper, the HWJC process was employed to remove alpha case layer (650~750 μm in thickness) from Ti-6Al-4V substrate. High jet traverse speeds were applied to both AWJ and PWJ passes to ensure the machining efficiency. The effects of abrasive size and some key process parameters of the PWJ operation on grit embedment and surface morphology were investigated. This paper seeks to:

- Validate the HWJC process as an effective innovative approach for removing thick alpha case with very little grit contamination.
- Investigate the influence of key process parameters of the PWJ operation on grit embedment and surface characteristics.

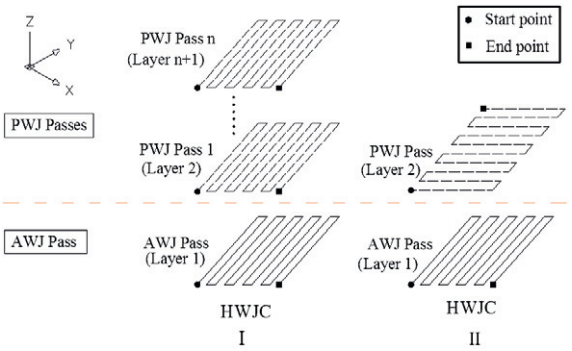

Fig.1. Examples of the HWJC process with different machining strategies (I) multiple PWJ passes using a same jet path as AWJ; (II) one PWJ pass using a different jet path.

2. Experimental setup and methods

2.1. Materials

The starting material was a Ti-6Al-4V sheet with an alpha case; samples were in sheet form with thickness of 5.5 mm and width of 20 mm. The thickness of alpha case contamination on both sides was between 650 μm to 750 μm (as shown in Fig.2). The microstructure of alpha case can also be seen in Fig.2.

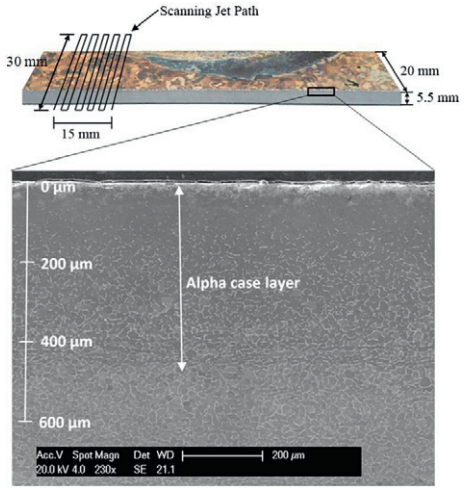

Fig. 2 Photograph of the alpha case workpiece and SEM image showing the cross-section of the alpha case.

2.2. Experimental Procedure

Experimental trials were carried out on an Ormond 5-axis AWJ machining system with a KMT Streamline SL-V100D ultrahigh pressure intensifier pump. A working head assembly with a 0.3 mm diameter sapphire orifice and a Rotec 100 tungsten carbide round-jet nozzle (1.5 mm in bore diameter) was used for both the AWJ and PWJ processes. A scanning jet path with 0.375 mm of step over (SO) covering a 30 mm × 15 mm area was employed for both AWJ and PWJ passes (as illustrated in Fig.2). Australian GMA garnet abrasives (mesh size 80) were used in the AWJ process. A Talysurf CLI1000 laser profiler was employed to measure the removal depth and surface roughness of the treated surfaces. An average value from five measurements was used to determine the depth of removal and surface roughness. A Philip XL30 FEG-SEM scanning electron microscopy with Oxford Instruments Link ISIS 300 series X-ray microanalyser was used to observe the morphology of the treated surfaces as well as quantify the amount of embedded grit. Image J software was employed for image processing (allowing automatic identification of grit particles from BS SEM images). All measurements of the level of grit embedment were conducted before and after PWJ operation for comparison.

2.3. Experimental setup

The primary objective of this study was to investigate the effects of PWJ process parameters on grit removal and surface characteristics; accordingly, a standard set of AWJ process parameters were employed with a range of PWJ process parameters. Table 1 summarizes the range of operating parameters in groups (I-VI). Each group of experiments sought to investigate the role of one process variable as shown in the shaded cells in Table 1.

2.4. Method of Grit Embedment Analysis

Current technologies for quantitative analysis of grit embedment include EDX composition analysis, X-ray mapping and BS image analysis. A preliminary study was carried out on seven selected samples which exhibited different degrees of grit contamination in order to compare the performance of these techniques. Results showed that X-ray mapping and BS image analysis compared favorably, showing that the difference in area percentage of grit presented on surfaces was within 5%. However, X-ray mapping requires long scanning times (8~10 minutes for each area) to get accurate maps. EDX composition analysis can only provide atomic percentage or weight percentage of garnet to indicate the grit embedment levels rather than provide a map of the distribution of the embedded grit as the other two methods. In light of this, BS image analysis was selected for this study due to its combination of simplicity and accuracy.

The contrast in backscattered (BS) images results from differences in mean atomic number of the materials being examined. Fig.3 shows an example of secondary electron and backscattered images of the same region on a HWJC-treated surface. In the BS image, titanium has a high brightness due to its higher mean atomic number whilst the garnet appears black or dark grey, due to its lower mean atomic number; this identification was confirmed by EDX spot analysis. The BS image also displays the contour of the surface topography showing as light grey streaks or isolated spots. It can be seen in Fig.3 that garnet particles and titanium can be distinguished more easily from the BS image than the SE image. Boxes in Fig.3 group the embedded grit into two types in terms of their grey-level in the BS image. Type-I embedded grit is visible as black in the BS image while Type-II grit appears a dark grey regions. The difference in color is likely to be due to the rough surface topography [7]. Type-II particles are embedded at surface depressions. Thus, the surrounding material tends to partially block the X-ray leading to the Type-II embedded particles charging up less than Type-I embedded particles which are lightly embedded and is not covered by surrounding material.

Table 1. Operating Parameters for the HWJC process

Parameters	I		II		III		IV		V		VI	
	AWJ	PWJ	AWJ	PWJ	AWJ	PWJ	AWJ	PWJ	AWJ	PWJ	AWJ	PWJ
Pressure (MPa)	345	345	345	345	345	345	345	345	345	345	345	345
SOD (*mm*)	30	20~70	30	20	20	10	20	10	20	10	10	5-20
v (*mm/min*)	3000	700	3000	500~1500	3000	2000	3000	2000	3000	2000	3000	2000
θ	90	90	90	90	90	90	90	30-90	90	90	90	90
n	1	1	1	1	1	1	1	1	1	1-8	1	2,3
f_a (*g/min*)	23	—	23	—	23	—	23	—	23	—	23	—
Mesh size	80#	—	80#	—	80#	—	80#	—	80#	—	80#	—
Jet path	S	S	S	S	S	S, CS*	S	S	S	S	S	S

*S—scanning path; CS—cross scanning path which is cross to the scanning path.

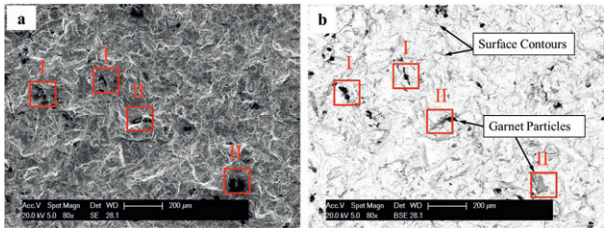

Fig.3 Illustration of grit embedment on a HWJC-treated surface: (a) SE image; (b) BS image. Boxes highlight garnet particles shown as dark or dark grey areas in the BS image

Based on the grit identification method discussed, the area percentage of embedded garnet particles (AG) can be calculated from the BS image by filtering out the white titanium and the light grey contours using Image J software, by setting a suitable threshold. As the accuracy of this method is highly dependent on the BS images, in order to maintain the accuracy, BS images of all HWJC-treated surfaces were taken with the same SEM setting (shown in Table 2). Images that were used for the grit embedment analysis in this study were taken at a magnification of 80 times. Higher magnifications were not selected since high magnification images may just interpret a local distribution of grit embedment rather than the average distribution over a wide area. Before the SEM investigation, all specimens were cleaned by immersion in an ultrasonic bath for 5 minutes at an intensity of 30W in order to remove loose contamination from the surface. The specimens were subsequently rinsed in de-ionized water and dried in air.

Table 2 SEM settings for BS image analysis

SEM Setup	Values
Beam Voltage	20 keV
Spot Size	5 nm
Working Distance	28 mm
Contrast	92.2
Brightness	47.8

3. Results

3.1. *Effects of PWJ Parameters on Grit Embedment and Surface roughness*

The effects of the PWJ parameters on the effectiveness of grit removal are shown in Fig.4. Fig.4(I) shows the area percentage of garnet on HWJC-treated surfaces as a function of PWJ SOD. PWJ with a SOD of 30 mm resulted in the lowest level of grit contamination with an area fraction of garnet of 9.5% (half of that before the PWJ pass) while SODs above 50 mm were significantly less effective in removal of embedded grit. The PWJ operation also resulted an increase in depth of material removed from the surface (about 50 μm to 220 μm); the maximum depth of removal in the PWJ operation was observed at a SOD of 20 mm. All HWJC-treated surfaces generally exhibited a slightly lower Ra than the surfaces treated by AWJ only. The lowest Ra value was 7.6 μm at SOD of 40 mm. The results indicate that after PWJ processing, the surface roughness was reduced by more than 20%, while the area fraction of grit was reduced to half of that before the PWJ operation.

The effect of jet traverse speed on grit removal in the HWJC process is shown in Fig. 4(II). It can be observed that grit embedment was reduced to as low as 6% at the lowest traverse speed of 500 mm/min. With an increase of traverse speed, the area fraction of garnet increased until it reached a peak value of 11% at a traverse speed of 700 mm/min. Further increases in the jet traverse speed lead to a decrease in grit embedment. The lowest grit contamination level was 3.8% at a traverse speed of 1500 mm/min. This was approximately one sixth of that before the PWJ operation. The depth of removal associated with the PWJ treatment was between 50 μm and 110 μm. The surface roughness of all HWJC-treated surfaces was slightly reduced by the PWJ treatment. The lowest Ra value was 8.3 μm at the traverse speed of 700 mm/min.

In order to investigate the possible effects of jet path design on the grit removal performance, two tool paths for the PWJ operation were compared. One used an identical path to the AWJ operation, while the other used a scanning path which was perpendicular to the jet path for the AWJ (cross-scanning path). The result is shown in Fig.4 (III). It is evident that PWJ with a cross scanning path resulted in a much lower grit embedment area (approximately one third of that using the scanning path identical to the AWJ) and slightly lower surface roughness, but little difference in the removal depth.

The effect of jet impingement angles of the PWJ operation is shown in Fig. 4(IV). It can be seen that a 90° jet impingement angle was the most efficient in terms of grit removal compared to other jet angles at the same SOD. At higher jet angles (60° and 75°), backward jet movement resulted in more efficient grit removal than forward movement. However, significant advantage in grit removal at the angle of 45° was observed with forward movement. At the lowest jet angle of 30°, there was no significant difference between backward and forward jet motion in terms of grit embedment. Jet impingement at a forward 45° resulted in the smallest removal depth. As jet angle increased, the surface roughness generally decreased, irrespective of backward or forward movement.

Fig. 4(V) shows that as the number of PWJ passes increases, the area coverage of embedded grit generally decreases. The lowest level of grit embedment (5% of grit coverage) was observed following five PWJ passes. The removal depth associated with the PWJ was only 10 μm after one PWJ pass. Ra was broadly unchanged.

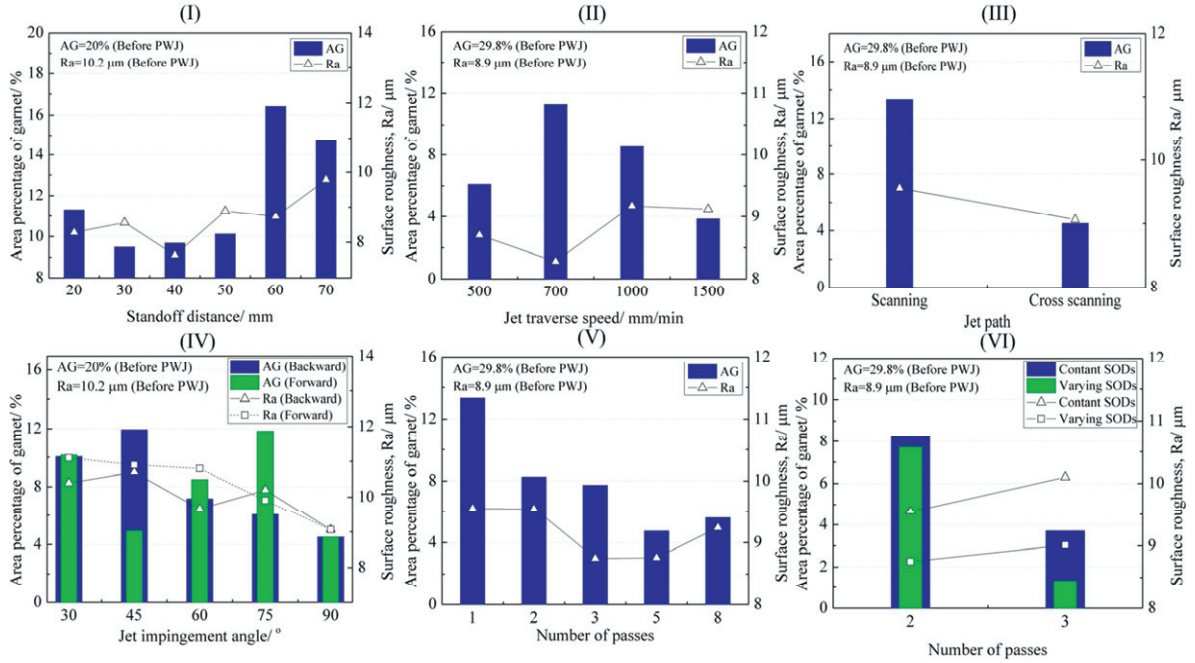

Fig. 4 Influence of PWJ parameters on the grit removal performance.

Fig. 4(VI) reveals that if multiple PWJ passes are applied, the selection of standoff distance for each PWJ pass also has significant influence on the performance of grit removal. It can be seen that for surfaces treated with the same number of PWJ passes, PWJ passes with varying SODs exhibited better performance than that with a constant SOD.

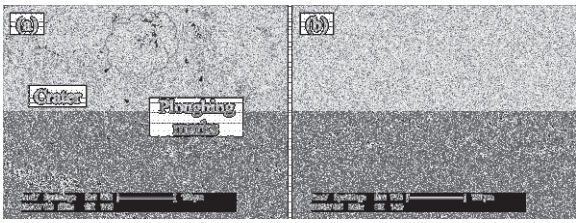

Fig. 5 SEM images of the (a) AWJ-treated surface; and (b) HWJC-treated surface.

3.2. *Surface Morphology of HWJC-treated Surface*

Fig. 5 shows SEM observations of AWJ and HWJC-treated surfaces. Ploughing and cutting marks from abrasive particles attack can be observed in Fig.5a. Crater-like indentation which results from direct impact of particles at high impact angles can be also observed occasionally. These craters tend to result in increases in the surface roughness. In contrast, Fig.5b displays the morphology of the same surface after PWJ cleaning. The surface was reshaped and exhibited features associated with ductile fracture.

4. Discussion

Results of this study demonstrate that the HWJC process can significantly reduce the level of embedded grit; the associated PWJ parameters influence the effectiveness of grit removal, the surface roughness, and the surface morphology. In order to understand this, it is necessary to understand the process of grit embedment.

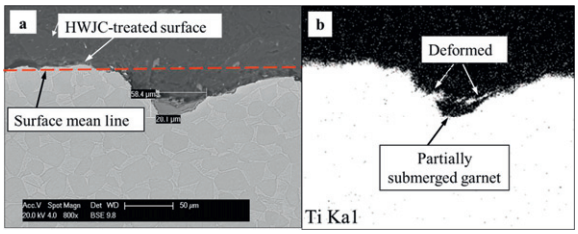

Fig. 6 Cross-section view of a submerged garnet fragment on a HWJC-treated Titanium alpha case surface (a) BS image; (b) X-ray map of Ti.

There are generally two types of embedment, namely deposited particles and submerged particles. Hashish [12] showed that submerged grit particles are difficult to remove, although deposited grit can be easily removed. Fig.6 shows a submerged grit particle observed in a HWJC-treated surface. It is clearly visible in Fig.6b that the grit is embedded at the bottom of a crater and covered by deformed titanium which may ‘protect’ the embedded particle from being removed in the PWJ cleaning process due to mechanical interlocking.

Therefore, sub-surface grit removal is prevented unless the PWJ is powerful enough to remove the titanium alloy around the particle and subsequently dislodge it.

The existence of an optimum SOD for waterjetting processes has been reported by Wang [13] who correlated this to the effective jet zone. The optimum SOD can explain the results shown in Fig. 4(I). It is interesting that Fig. 4(II) showed that the effectiveness of grit removal performance is not simply energy density-dependent as lower traverse speeds (corresponding to higher energy densities) did not always result in a lower level of grit contamination. However, the effect of PWJ impingement angle and number of passes on the grit removal performance (as shown in Fig.4(IV) and (V)) indicated that as the energy density increases, the resulting AG% decreases.

It has been shown that PWJ cleaning with a scanning path which is perpendicular to that of the AWJ operation was more effective at grit removal than that using the same path (Fig. 4(III)), while the material removal depths of material using the two PWJ paths are similar. As the depth of removal is determined by the deepest valley of the mean profile of the treated area, it is proposed that the more effective grit removal using the cross tool path results from it being more effective in removal of peak areas due to lateral outflow jetting. Thus, the embedded particles in these peak areas can be subsequently removed. The results shown in Fig. 4(VI) may be explained in light of PWJ passes at different SODs being less likely to leave lay marks on the surface. Thus, embedded grit particles have more chance of being exposed to PWJ droplet impacts.

The results presented also showed that there is no determinate relationship between grit embedment level and surface roughness. Lower levels of grit embedment were not always associated with lower surface roughness. An embedded particle may be partly submerged in the AWJ treated surface; such a particle may be only partially removed under subsequent PWJ impact, leaving the submerged fragment in the surface due to mechanical interlocking (as shown in Fig. 6a). The fragment occupies the indentation which makes the surface flat. Herein it may contribute to a decrease in Ra. However, if the PWJ impulse is powerful enough to crush the entire embedded grit, the embedded particle can be entirely removed, leaving the crater unoccupied. This could again cause an increase in Ra.

5. Conclusion

Based on the results from this study, it can be concluded that the proposed HWJC process can effectively remove a thick alpha case layer with a much lower degree of grit contamination than an AWJ only process. However, the embedment behavior of abrasives affects their ability to be removed under PWJ impingement. The operating parameters of PWJ in HWJC also play significant roles in the effectiveness of grit removal. The PWJ operation with applied high speed traverse speeds resulted in less erosion of the substrate and also had limited influence on the surface roughness. There was no determinate relationship between PWJ parameters and surface roughness within the experimental conditions since the presence and absence of embedded grit can modify the roughness profile of the surface.

References

1. Singh, J. and S.C. Jain, *Mechanical Issues in Laser and Abrasive Water-Jet Cutting*. Jom-Journal of the Minerals Metals & Materials Society, 1995. **47**(1): p. 28-30.
2. Chen, F.L., et al., *Minimising particle contamination at abrasive waterjet machined surfaces by a nozzle oscillation technique.* International Journal of Machine Tools and Manufacture, 2002. **42**(13): p. 1385-1390.
3. Chillman, A., et al., *High Pressure Waterjets - An Innovative Means of Alpha Case Removal for Superplastically Formed Titanium Alloys.* Superplasticity in Advanced Materials, 2010. **433**: p. 103-111.
4. Kong, M.C., D. Axinte, and W. Voice, *Aspects of material removal mechanism in plain waterjet milling on gamma titanium aluminide.* Journal of Materials Processing Technology, 2010. **210**(3): p. 573-584.
5. Kong, M.C., D. Axinte, and W. Voice, *An innovative method to perform maskless plain waterjet milling for pocket generation: a case study in Ti-based superalloys.* International Journal of Machine Tools and Manufacture, 2011. **51**(7-8): p. 642-648.
6. Amada, S., T. Hirose, and T. Senda, *Quantitative evaluation of residual grits under angled blasting.* Surface & Coatings Technology, 1999. **111**(1): p. 1-9.
7. Arola, D. and C.L. Hall, *Parametric effects on particle deposition in abrasive waterjet surface treatments.* Machining Science and Technology, 2004. **8**(2): p. 171-192.
8. Boud, F., et al., *Abrasive waterjet cutting of a titanium alloy: The influence of abrasive morphology and mechanical properties on workpiece grit embedment and cut quality.* Journal of Materials Processing Technology, 2010. **210**(15): p. 2197-2205.
9. Maruyama, T., K. Akagi, and T. Kobayashi, *Effect of the Blasting Angle on the Amount of the Residual Grit on Blasted Substrates*.
10. Maruyama, T., K. Akagi, and T. Kobayashi, *Effects of Blasting Parameters on Removability of Residual Grit*. Journal of Thermal Spray Technology, 2006. **15**(4): p. 817-821.
11. Tsai, F.C., et al., *An investigation into superficial embedment in mirror-like machining using abrasive jet polishing*. International Journal of Advanced Manufacturing Technology, 2009. **43**(5-6): p. 500-512.
12. Hashish, M., *Characteristics of surfaces machined with abrasive-waterjets.* Journal of Engineering Materials and Technology, 1991. **113**: p. 354-362.
13. Wang, J., *Abrasive Waterjet Machining of Polymer Matrix Composites – Cutting Performance, Erosive Process and Predictive Models.* The International Journal of Advanced Manufacturing Technology, 1999. **15**(10): p. 757-768.